Available online at www.sciencedirect.com
ScienceDirect
Journal of Solid State Chemistry 180 (2007) 834–839
JOURNAL OF SOLID STATE CHEMISTRY
www.elsevier.com/locate/jssc

Crystal structure and magnetic properties of the solid-solution phase $Ca_3Co_{2-v}Sc_vO_6$

Charles H. Hervoches[a,*], Vivian Miksch Fredenborg[b], Arne Kjekshus[b], Helmer Fjellvåg[b], Bjørn C. Hauback[a]

[a]*Institute for Energy Technology, N-2007 Kjeller, Norway*
[b]*Centre for Materials Science and Nanotechnology, Department of Chemistry, University of Oslo, N-0315 Oslo, Norway*

Received 31 August 2006; received in revised form 24 November 2006; accepted 1 December 2006
Available online 12 December 2006

Abstract

The two crystallographically non-equivalent Co atoms of the quasi-one-dimensional crystal structure of $Ca_3Co_2O_6$ form chains with alternating, face-sharing polyhedra of $Co2O_6$ trigonal prisms and $Co1O_6$ octahedra. This compound forms a substitutional solid-solution phase with Sc, in which the Sc atoms enter the Co2 sublattice exclusively. The homogeneity range of $Ca_3Co_{2-v}Sc_vO_6$ (more specifically $Ca_3Co1Co2_{1-v}Sc_vO_6$) extends up to $v \approx 0.55$. The crystal structure belongs to space group $R\bar{3}c$ with lattice parameters (in hexagonal setting): $9.0846(3) \leqslant a \leqslant 9.1300(2)$ Å and $10.3885(4) \leqslant c \leqslant 10.4677(4)$ Å. The magnetic moment decreases rapidly with increasing amount of the non-magnetic Sc solute in the lattice.

Keywords: Scandium substitution; $Ca_3Co_2O_6$ structure; Low-dimensional material; Magnetic properties

1. Introduction

The quasi-one-dimensional oxide $Ca_3Co_2O_6$ and the related materials $M_3TT'O_6$ (M = Ca, Sr; T and T' transition metals) have attracted considerable interest in recent years, due to their peculiar magnetic properties [1] and large thermoelectric powers [2]. $Ca_3Co_2O_6$ is isotypic with K_4CdCl_6 [3] (or in the present context perhaps rather related to the crystal structure of the $M_3TT'O_6$ phases) (space group $R\bar{3}c$, $a = 9.0793(7)$ Å, $c = 10.381(1)$ Å [4] in hexagonal setting). Two non-equivalent cobalt atoms coexist in the characteristic quasi-one-dimensional chains of the structure forming alternating face-sharing $Co1O_6$ octahedra (o) and $Co2O_6$ trigonal prisms (t).

The highly peculiar structure is responsible for notable anisotropic magnetic properties. Along the chains, the magnetic moments at the $Co2^t$ sites are ordered ferromagnetically (F), but one out of three chains is antiferromagnetically (AF) coupled, resulting in an overall ferrimagnetic (Ferri) structure below $T_c \approx 25$ K [4,5]. There are several reports of substitution at the $Co1^o$ site (e.g., $Ca_3MnCo2O_6$ with long-range AF magnetic ordering at low temperatures [6–8]), whereas to the best of our knowledge appreciable substitution on the $Co2^t$ site has hitherto not been established.

Partially disordered AF has been reported [9] for $Ca_3RhCo2O_6$, whereas a similar magnetic behavior was not observed [10] for $Ca_3IrCo2O_6$. $Ca_3RuCo2O_6$ has been reported [10] to exhibit ordinary AF behavior. A change in the sign of the Weiss constant (θ) has been reported for $Ca_3Co_{1+v}Ir_{1-v}O_6$ and this has been linked to a monoclinic distortion of the structure [11,12]. Only small amounts of Cr appear to have been introduced on the $Co1^o$ site by traditional solid-state synthesis, but this substitution has nevertheless a great effect on the magnetic properties [13]. Similar observations have been made for samples with small amounts of Fe on the $Co2^t$ site [14,15].

The present paper reports on the structural characterization and magnetic properties of the $Ca_3Co_{2-v}Sc_vO_6$ phase.

*Corresponding author. Fax: +47 63 81 63 56.
E-mail address: Charles.Hervoches@ife.no (C.H. Hervoches).

0022-4596/$ - see front matter © 2006 Elsevier Inc. All rights reserved.
doi:10.1016/j.jssc.2006.12.007

2. Experimental section

All samples were synthesized by the citrate-gel technique following the procedure described in Refs. [4,5]. The starting materials were $CaCO_3$ (p.a., Merck), $Co(CH_3COO)_2 \cdot 4H_2O$ (>99%, Fluka), Sc_2O_3 (99%, Koch-Light), and citric acid monohydrate [$(HOOC)CH_2C(OH)(COOH)CH_2(COOH) \cdot H_2O$; reagent grade, Sturge biochemicals] together with distilled water. The obtained citrate gel was dehydrated at 150 °C overnight and organic constituents were removed by incineration at 450 °C for a few hours. Finally, the samples were pressed into pellets and heat treated at 1000 °C for 1 week with intermediate grinding.

At this point, we like to mention a sample for which the intention was to substitute 10% of Ca by Sc. Analyses of the product of this synthesis proved that Sc has effectively substituted for Co instead of Ca, and the resulting material turned out to be $Ca_3Co_{1.7}Sc_{0.3}O_6$ with Co_3O_4 as a second phase.

The reaction products were characterized at room temperature by powder X-ray diffraction (PXD) using a Guinier–Hägg camera with monochromatized Cu$K\alpha_1$ or Cr$K\alpha_1$ radiation and Si as internal standard.

Powder neutron diffraction (PND) data were collected with the high-resolution powder neutron diffractometer PUS at the JEEP II reactor, Kjeller, Norway. Cylindrical vanadium sample holders were used. Monochromatic neutrons with wavelength $\lambda = 1.5554$ Å were obtained from a Ge(511) focusing monochromator. The detector unit consists of two banks of seven position-sensitive ^{3}He detectors, each covering 20° in 2θ. Intensity data were collected from $2\theta = 10$ to 130° in steps of $\Delta(2\theta) = 0.05°$. Temperatures between 7 and 298 K were obtained by means of a Displex cooling system. A Lake Shore DRC 82C controller was used, and the temperature was measured and controlled by means of a silicon diode. Structure determination and profile refinement were performed using the Rietveld refinement program Fullprof.98 [16].

Magnetic susceptibility data were recorded in the zero-field-cooled (ZFC) mode with an MPMS magnetometer (Quantum Design) between 5 and 300 K for applied magnetic fields (H) from 25 to 1000 Oe. Field cooled (FC) experiments were performed for $H = 1$ kOe. Magnetization data at 5 K were recorded for fields up to 50 kOe. Saturation magnetization was estimated by $1/H$ extrapolation.

3. Results and discussion

3.1. Crystal structure

The room-temperature crystal structure of single-phase samples of $Ca_3Co_{2-v}Sc_vO_6$ equals that of the parent-material $Ca_3Co_2O_6$. The results show unequivocally that Sc can partly substitute $Co2^t$ in $Ca_3Co_2O_6$. Fig. 1 shows that

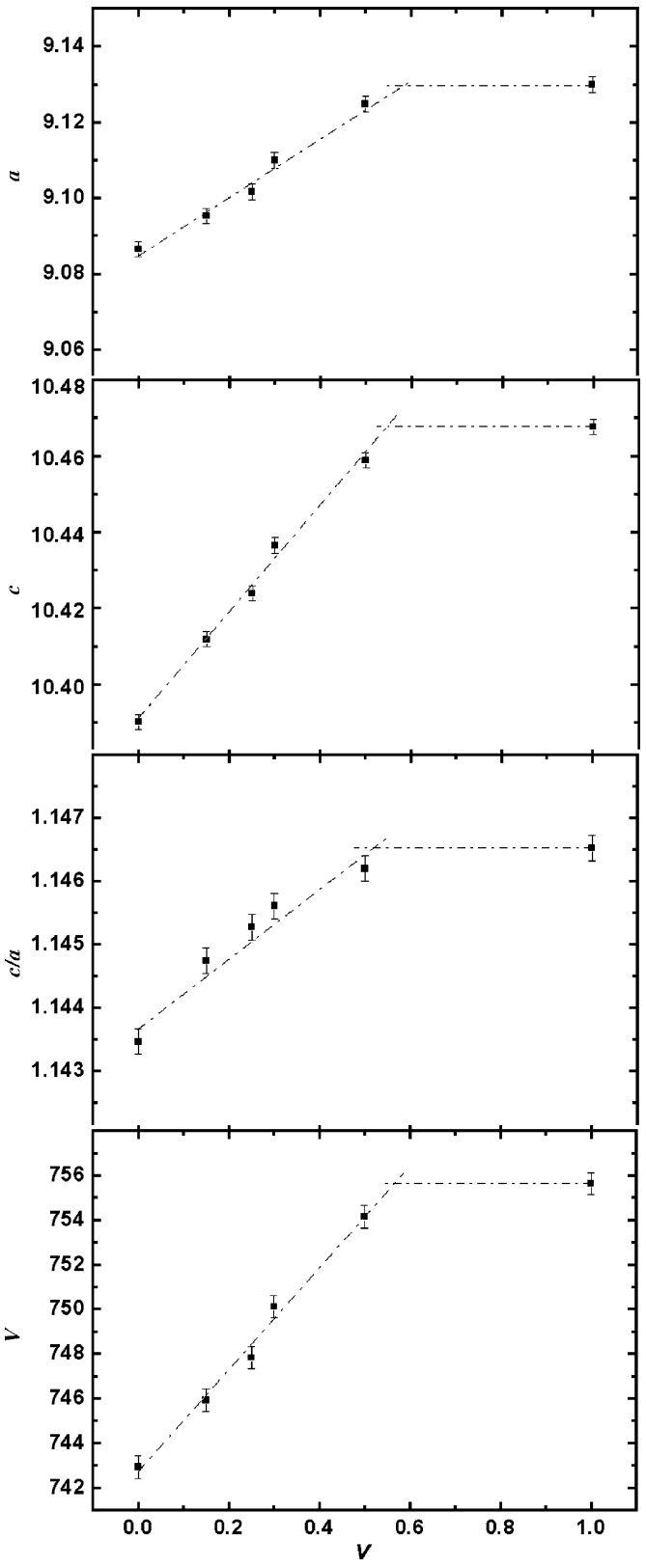

Fig. 1. Evolution in unit-cell dimensions (a and c in Å, c/a, and volume (V) in Å^3) with the substitution parameter v of $Ca_3Co1^oCo2^t_{1-v}Sc_vO_6$. The sample with nominal composition $v = 1$ comprised three phases.

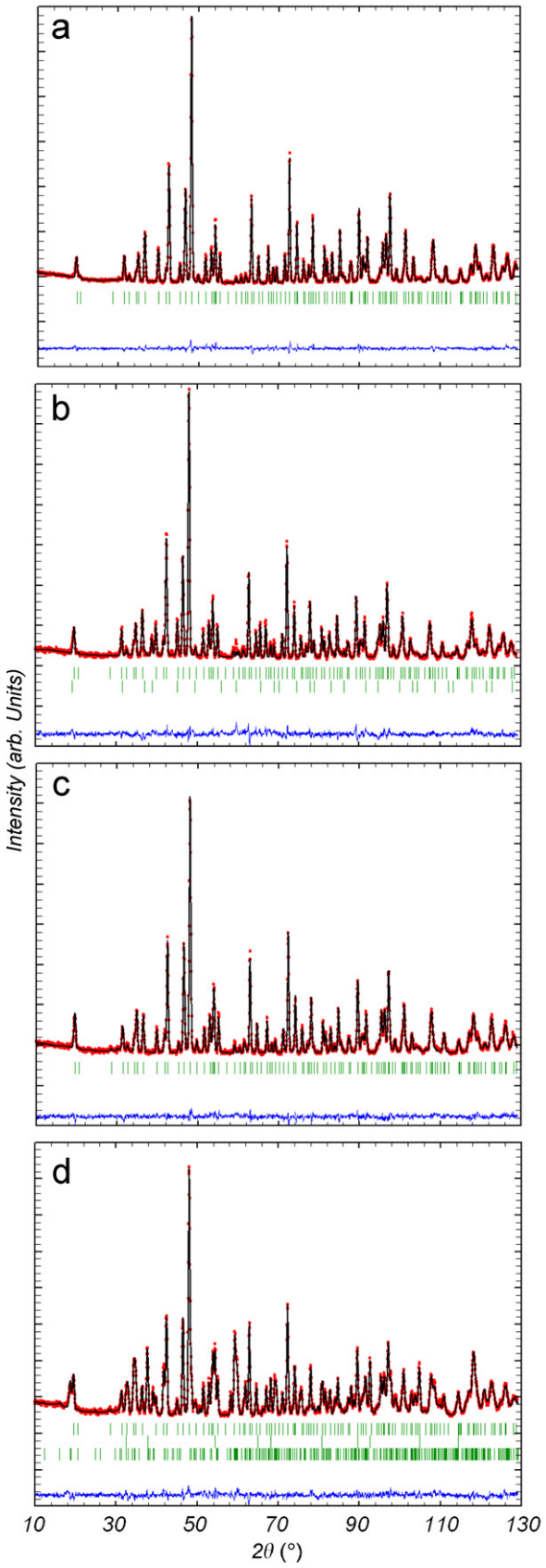

Fig. 2. Observed (points), calculated (tracing), and difference (lower profile; on the same scale) powder neutron diffraction patterns for $Ca_3Co1^oCo2^t_{1-v}Sc_vO_6$ at 298 K for samples with (a) $v = 0.25$, (b) $v = 0.30$, (c) $v = 0.50$, and (d) $v = 1$ (three-phase sample).

phase-pure materials (of samples annealed at 1000 °C) can be obtained in the range $0 \leqslant v < \sim 0.55$, which thus defines the solid-solution range of the $Ca_3Co_{2-v}Sc_vO_6$ phase. Attempts to synthesize materials with higher amounts of Sc ($\sim 0.55 < v \leqslant 1$) result in the occurrence of undesired impurities such as CaO and/or $CaSc_2O_4$. The structure refinements of the 298 K PND data gave a Sc content of $v = 0.47$ for the sample with nominal composition $v = 0.50$. However, importance was not attached to this apparent discrepancy since there are possible sources of error in the PND data base as well as in its computational treatment. Moreover, the evolution in unit-cell dimensions, interatomic distances, and magnetic moments with v (see below) unequivocally show that the nominal Sc content also is the actual composition of the $v = 0.50$ sample. For the samples with nominal compositions $0 \leqslant v \leqslant 0.30$ only negligible deviations in the composition parameter v were obtained by the structure refinements. Significant amounts of oxygen defects were not detected in the refinements, and the oxygen content of 6 per formula unit was accordingly accepted without further analyses. As expected the volume of the structure increases on Sc-for-Co substitution (Fig. 1) due to the appreciably larger size of Sc.

Refinements of the room-temperature PND data were performed using the parent $Ca_3Co_2O_6$ structure as the starting point. Attempts were first made to refine the structure of the solid-solution phase with Sc in the octahedral (6*a*) position as already established for the Ca_3CoMnO_6 phase [6–8]. These attempts failed and since, moreover, substitution of Sc for Ca could be ruled out (see Section 2; also confirmed by refinements) the attention was focused on substitution at the $Co2^t$ site. These refinements immediately gave a good agreement between observed and calculated difference patterns at 298 and 8 K (Figs. 2 and 3). The refined structural parameters are given in Table 1.

The fact that Sc substitutes exclusively for $Co2^t$ is most likely due to the size of the substitute [$r(Sc^{3+}) = 0.75$ Å; CN = 6 [17]] which probably is of wrong size for the Ca and $Co1^o$ sites. As a matter of fact, bond-valence-sum [18] analysis gives a value of ~3.2 for substitution at the $Co2^t$ site, whereas a very unfavorable value of ~5.0 would have been associated with accommodation of Sc at the smaller $Co1^o$ site.

The variation of selected interatomic distances with v is shown in Fig. 4. The introduction of Sc in the structure induces a smooth increase in the $Co1^o$–O and $Co2^t$–O distances, from 1.9137(16) Å for $v = 0$ to 1.9210(12) Å for $v = 0.50$ for $Co1^o$–O and from 2.0660(15) Å for $v = 0$ to 2.0852(12) Å for $v = 0.50$ for $Co2^t$–O (Fig. 4). The intrachain Co1–Co2/Sc distances ($c/4$) increase also smoothly, from 2.5971(1) Å for $v = 0$ to 2.6147(1) Å for $v = 0.50$. These variations in the interatomic distances are brought about by the larger size of Sc^{III} (0.75 Å) compared with Co^{III} (0.61 Å, according to Ref. [17]; actually somewhat larger for the high-spin state of $Co2^t$, see Refs. [5,19]). Since there occur no dramatic changes in the structural data upon the Sc insertion, we can conclude that it seems

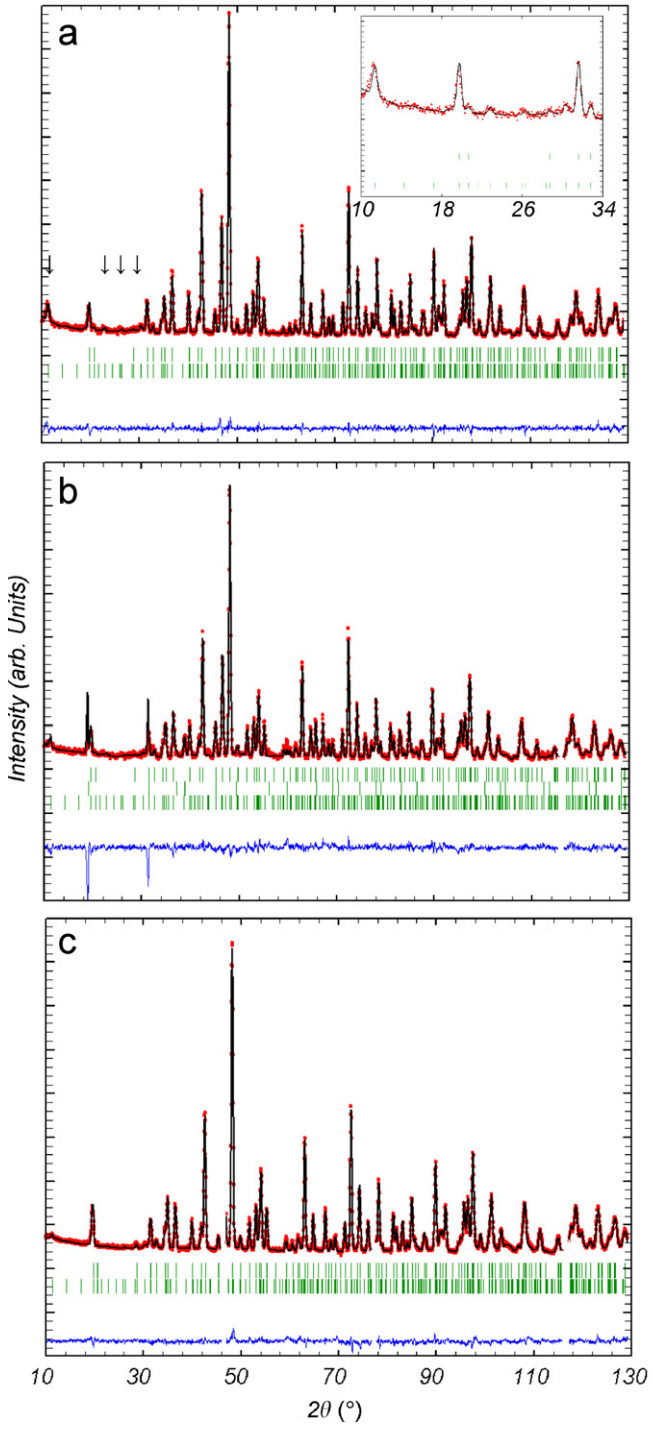

Fig. 3. Observed (points), calculated (tracing), and difference (lower profile; on the same scale) powder neutron diffraction patterns for $Ca_3Co1^oCo2^t_{1-v}Sc_vO_6$ at (a) 8 K for $v = 0.25$, (b) 10 K for $v = 0.30$, and (c) 7 K for $v = 0.50$. Reflections due to magnetic ordering are marked by arrows in part a, which also shows an inset with a zoom of these reflections.

reasonable to maintain that the valence and spin states of $Co1^o$ and $Co2^t$ remain unchanged.

An interesting aspect of the Sc-substituted phase is that the solid solubility only extends to $v \approx 0.55$ as opposite to the corresponding substitution phases with, say, Mn [6–8], Rh [9], and Ir [12] which is reported to substitute at the $Co1^o$ site up to $v \approx 1.0$. We believe that this distinction is not rooted in fundamental bond-associated features for the cobalt atoms in octahedral and/or trigonal-prismatic sites. It rather reflects the number of $Co1^o$–$Co2^t$ bonds that can be tolerated broken by insertion of a solute that lacks d orbitals which appear to be crucial for the $Co1^o$–$Co2^t$ bonds and thus the stability of the $Ca_3Co_2O_6$ atomic arrangement. It should also be noted that the Sc-for-Co substitution may be somewhat hampered by size mismatch, since the radii concerned probably balance on the very edge of Hume-Rothery's [20] empirical 15%-size rule.

3.2. Magnetic properties

Detailed mapping of the temperature dependence of the magnetic susceptibility was made from 5 to 300 K for $v = 0$, 0.25, 0.30, and 0.50. As seen from the caption to Fig. 5, both the paramagnetic moment (μ_p) and the Weiss constant (θ) decrease with increasing Sc content. The magnetization versus applied magnetic field (H) at 5 K for the $v = 0.25$ sample (Fig. 6) shows a small hysteresis loop and a tendency to saturation at the highest field strengths.

PND measurements for the samples with $0 \leqslant v \leqslant 0.50$ were performed at low temperature to establish magneto-structural consequences of the Sc-for-$Co2^t$ substitution. Low-temperature PND data were not collected for the three-phase sample with $v = 1$. In accordance with observations for the parent compound $Ca_3Co_2O_6$, additional Bragg reflections due to Ferri ordering (see introduction) appear in the low-temperature PND patterns for samples with $v \leqslant 0.50$ (Fig. 3).

The magnetic ordering temperature for the $v = 0.25$ sample was established at $T_c \approx 15(1)$ K from the temperature dependence of the integrated intensity (Fig. 7) of the magnetic 1 0 0 reflection (at $2\theta = 11.3°$, see Fig. 2). Good conformity was found between the magnetic ordering temperatures determined by PND and magnetic measurements.

The magnetic structure of the $Ca_3Co_{2-v}Sc_vO_6$ phase was refined in space group $P\bar{1}$, with the parameters for the crystal structure constrained to correspond to the $R\bar{3}c$ description used for the refinements at 298 K. The obtained magnetic structure is identical with that of the parent material. The magnetic moments (oriented along [001]) are subject to intrachain F alignment supplemented with F and AF interchain couplings (viz. a $\uparrow\uparrow\downarrow$-moment arrangement).

The magnetic moment of $Co2^t$ decreases rapidly as increasing amounts of the non-magnetic Sc solute is introduced (Table 1 and Fig. 8), going from 2.96(5) μ_B for $v = 0$ to 1.7(1) μ_B for $v = 0.50$. There is no significant ordered moment for $Co1^o$ (Table 1). The introduction of Sc^{III} cuts the magnetic information channels along the ferromagnetic chains (see also the discussion for the $Ca_3Co_{2-v}Fe_vO_6$ phase in Ref. [15]). This mechanism

Table 1
Unit-cell dimensions, atomic coordinates, and magnetic moments along c as obtained by refinements of powder X-ray and neutron diffraction data for $Ca_3Co_{2-v}Sc_vO_6$

v	T (K)	a (Å)	c (Å)	x (Ca)	x (O)	y (O)	z (O)	M_c (Co1)	M_c (Co2)
				(18*e*)	(36*f*)	(36*f*)	(36*f*)		
0	298	9.0846(3)	10.3885(4)	0.3690(3)	0.1765(2)	0.0243(2)	0.1138(1)		
0	10	9.063(1)	10.369(1)	0.3696(3)	0.1769(2)	0.0237(3)	0.1145(2)	0.03(4)	2.96(5)
0.15	298	9.0953(2)	10.4118(2)	—	—	—	—		
0.25	298	9.1020(1)	10.4240(2)	0.3686(1)	0.17677(8)	0.02436(8)	0.11337(5)		
0.25	8	9.0749(1)	10.4000(2)	0.3692(2)	0.1774(1)	0.0242(1)	0.11337(8)	0.18(7)	2.19(9)
0.30	298	9.1103(3)	10.4366(4)	0.3691(3)	0.1767(2)	0.0240(2)	0.1128(1)		
0.30	10	9.0834(5)	10.4137(4)	0.3688(3)	0.1767(2)	0.0241(2)	0.1130(1)	–0.3(2)	2.0(1)
0.50	298	9.1247(2)	10.4588(3)	0.3687(2)	0.1768(1)	0.0243(1)	0.11297(9)		
0.50	7	9.1043(3)	10.4429(3)	0.3691(2)	0.1772(1)	0.0245(1)	0.11288(7)	–0.2(2)	1.7(1)
1[a]	298	9.1300(2)	10.4677(4)	0.3684(2)	0.1767(2)	0.0238(2)	0.1130(1)		

Space group $R\bar{3}c$ (hexagonal setting). Co1 and Co2/Sc are in sites 6*b* (0, 0, 0) and 6*a* (0, 0, 1/4), respectively.
[a]Three-phase sample; see text.

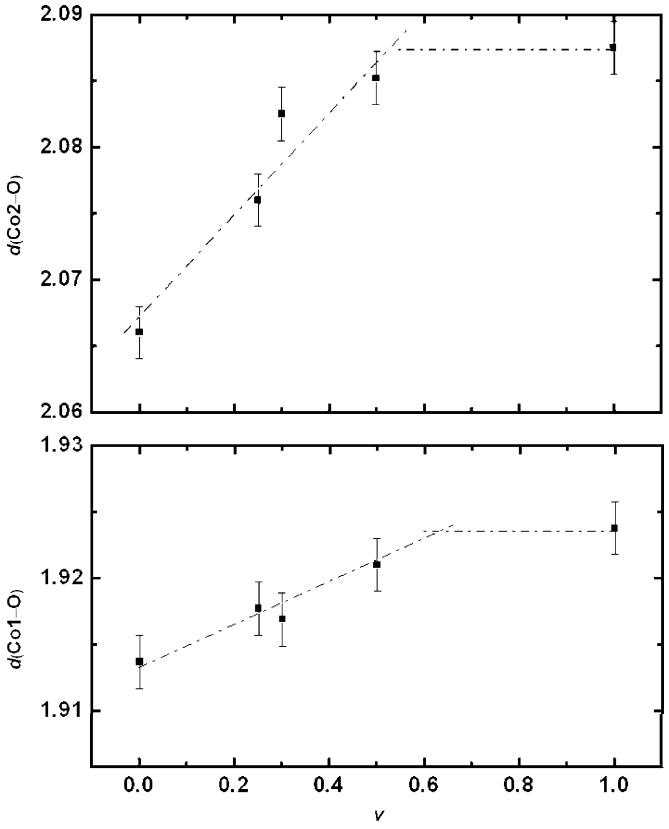

Fig. 4. Evolution of interatomic distances (in Å) $Co1^o$–O and $Co2^t$–O versus v in $Ca_3Co_{2-v}Sc_vO_6$ at 298 K as derived from refinements of PND data. The values for $v = 1$ refer to the three-phase sample with the said nominal composition.

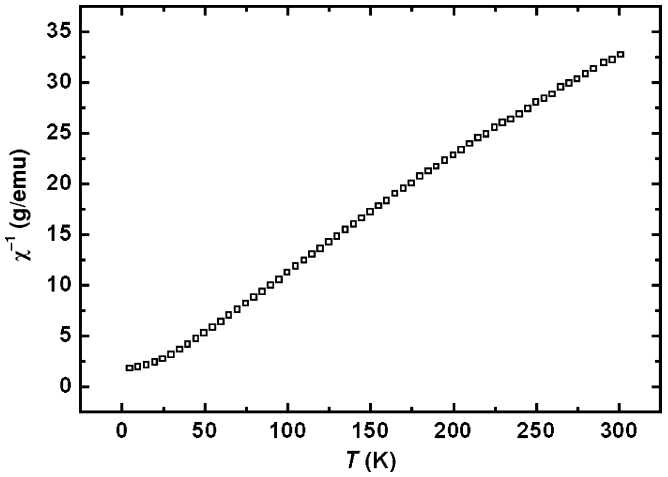

Fig. 5. Inverse magnetic susceptibility versus temperature for Ca_3Co1^o-$Co2^t_{1-v}Sc_vO_6$ with the $\chi^{-1}(T)$ relationship for $v = 0.25$ as example. Paramagnetic parameters for all carefully studied samples, according to susceptibility measurements; moments: $\mu_P = 5.5$, 4.9, 4.5, and 4.1 μ_B and Weiss constants: $\theta = 31.2$, −2.0, −1.7, and −3.0 K for $v = 0$, 0.25, 0.30, and 0.50.

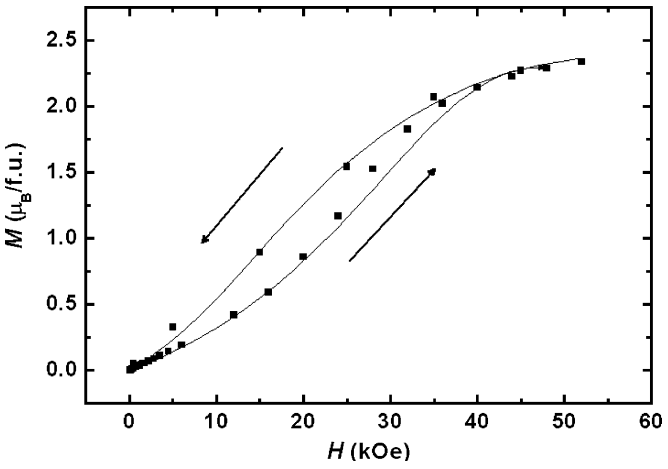

Fig. 6. Magnetization versus external magnetic field for $Ca_3Co1^oCo2^t_{0.75}Sc_{0.25}O_6$ recorded at 5 K. Curves are guides for eye.

rapidly lowers the magnetic moment at the $Co2^t$ site as well as the co-operative magnetic ordering temperature.

Extrapolation of the $M_c(Co2^t)$ versus v relation (Fig. 8) to the hypothetical phase limit $v = 1$ leads to a virtually zero rest moment (actually $M_c(Co2^t) \approx 0.2\,\mu_B$ at $v = 1$) which provides an additional clear evidence for the selectivity of the Sc-for-$Co2^t$ substitution. A corresponding extrapolation of spin quantum numbers calculated from

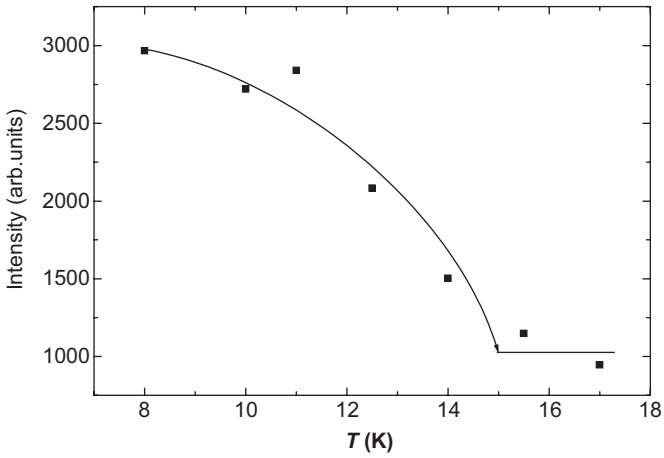

Fig. 7. Integrated intensity of the magnetic 1 0 0 reflection for Ca_3Co1^o-$Co2^t_{0.75}Sc_{0.25}O_6$ as function of temperature. Curve is guide for eye.

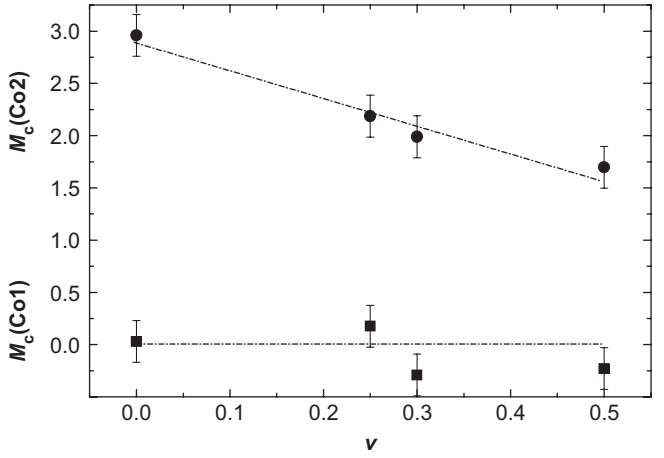

Fig. 8. Evolution of ordered magnetic moments (in μ_B along [0 0 1]) obtained from Rietveld refinements of the low temperature (8–10 K) PND data for $Ca_3Co1^oCo2^t_{1-v}Sc_vO_6$.

the μ_P data in the caption to Fig. 5 (according to the spin-only approximation) gives a rest spin of ~0.8. A confrontation of the findings for the paramagnetic and co-operative magnetic states indicates that a significant amount of unpaired electron density is associated with the $Co1^o$ and/or O atoms.

4. Conclusion

$Ca_3Co_2O_6$ forms a solid-solution phase with Sc in which the substitution exclusively takes place at the trigonal-prismatic Co site. The solid solubility ends at $v \approx 0.55$. The actual value of the phase limit reflects possibly the amounts of broken $Co1^o$–$Co2^t$ interactions the $Ca_3Co_2O_6$ structure can tolerate. Parallel with the decreasing stability of the atomic arrangement with increasing Sc content also the magnetic moment and co-operative magnetic ordering temperature rapidly decrease as effects of, respectively, dilution of the magnetic lattice and reduced magnetic exchange interaction.

Acknowledgment

This work has received support from The Research Council of Norway, grant 158518/S10 (NANOMAT).

References

[1] S. Aasland, H. Fjellvåg, B. Hauback, Solid State Commun. 101 (1997) 187.
[2] A. Maignan, S. Hébert, C. Martin, D. Flahaut, Mater. Sci. Eng. B 104 (2003) 121.
[3] G. Bergerhoff, O. Schmitz-Dumont, Z. Anorg. Allg. Chem. 284 (1956) 10.
[4] H. Fjellvåg, E. Gullbrandsen, S. Aasland, A. Olsen, B.C. Hauback, J. Solid State Chem. 124 (1996) 190.
[5] C.H. Hervoches, H. Fjellvåg, A. Kjekshus, V.M. Fredenborg, B.C. Hauback, J. Solid State Chem. (2006), in press, doi:10.1016/j.jssc.2006.10.037.
[6] V.G. Zubkov, G.V. Bazuev, A.P. Tyutyunnik, I.F. Berger, J. Solid State Chem. 160 (2001) 293.
[7] S. Rayaprol, K. Sengupta, E.V. Sampathkumaran, Solid State Commun. 128 (2003) 79.
[8] C.H. Hervoches, H. Okanoto, A. Kjekshus, H. Fjellvåg, B.C. Hauback, to be published.
[9] S. Niitaka, K. Yoshimura, K. Kosuge, M. Nishi, K. Kakurai, Phys. Rev. Lett. 87 (2001) 177202.
[10] S. Rayaprol, K. Sengupta, E.V. Sampathkumaran, Phys. Rev. B 67 (2003) 180404.
[11] H. Kageyama, K. Yoshimura, K. Kosuge, J. Solid State Chem. 140 (1998) 14.
[12] S. Rayaprol, K. Sengupta, E.V. Sampathkumaran, Proc. Indian Acad. Sci. 115 (2003) 553.
[13] D. Flahaut, A. Maignan, S. Hébert, C. Martin, R. Retoux, V. Hardy, Phys. Rev. B 70 (2004) 094418.
[14] H. Kageyama, S. Kawasaki, K. Mibu, M. Takano, K. Yoshimura, K. Kosuge, Phys. Rev. Lett. 79 (1997) 3258.
[15] J. Arai, H. Shinmen, S. Takeshita, T. Goko, J. Magn. Magn. Mater. 272–276 (2004) 809.
[16] J. Rodriguez-Carvajal, T. Roisnel, International Union of Crystallography, Newsletter 20, 1998.
[17] G. Aylward, T. Findley, SI Chemical Data, third ed., Wiley, Brisbane, 1994.
[18] N.E. Brese, M. O'Keeffe, Acta Crystallogr. Sect. B 47 (1991) 192.
[19] W.B. Pearson, The Crystal Chemistry and Physics of Metals and Alloys, Wiley, New York, 1972.
[20] W. Hume-Rothery, The Structure of Metals and Alloys, Institute of Metals, London, 1936.